Optimum Mitigation of distortion induced by Rayleigh Backscattering in Radio-over-Fiber links for the Square Kilometer Array Radio-Telescope

1st Jacopo Nanni
DEI-University of Bologna
Bologna, Italy
jacopo.nanni3@unibo.it

2nd Andrea Giovannini
DEI-University of Bologna
Bologna, Italy
andrea.giovannini10@studio.unibo.it

3rd Muhammad Usman Hadi
DEI-University of Bologna
Bologna, Italy
muhammadusman.hadi2@unibo.it

4th Simone Rusticelli
IRA-INAF
Medicina (Bologna), Italy
rusticel@ira.inaf.it

5th Federico Perini
IRA-INAF
Medicina (Bologna), Italy
f.perini@ira.inaf.it

6th Jader Monari
IRA-INAF
Medicina (Bologna), Italy
j.monari@ira.inaf.it

7th Enrico Lenzi
Protech S.a.S
Castelfranco Veneto (TV), Italy
e.lenzi@protechgroup.it

8th Giovanni Tartarini
DEI-University of Bologna
Bologna, Italy
giovanni.tartarini@unibo.it

Abstract—**This paper presents the theoretical and experimental study of unexpected distortions induced by the Rayleigh backscattering phenomenon in Radio-over-Fiber (RoF) links within the Square Kilometer Array (SKA) project. For this system, the radiofrequency (RF) signals coming from the sky and celestial sources are received by more than 130k antennas individually and then transmitted to the signal processing room through an analogue RoF link. The low frequency band considered (from 50MHz to 350MHz) and the relatively low levels of the power of such RF signals are identified as the cause of these distortion effects which can decrease drastically the receiver dynamic range. An analysis of the phenomenon is presented in this work, together with an efficient solution optimized for the considered applicative case.**

Keywords—Rayleigh Backscattering, Low Frequency Aperture Array, Square Kilometer Array, Radio-over-Fiber.

I. INTRODUCTION

The designing and construction of the Square Kilometer Array (SKA) represents one of the most challenging activities in view of the realization of future technologies of radio astronomic plants. This innovative system, composed of many antenna arrays for an equivalent collecting area larger than one square kilometer, will provide a sensitivity more than two orders of magnitude higher with respect to already existing radio astronomic plants [1].

Currently, the developing of phase-1 of the SKA project is taking place. Two systems will be realized operating at two different frequency bands: SKA1-LOW, to be developed in Australia, will work at frequencies ranging from 50MHz to 350MHz, while SKA1-MID, located in South Africa, will work at frequencies higher than 400 MHz. This paper focuses on the first one. In detail, SKA1-LOW is going to be composed on more than 130k antennas with 512 stations 256 sparse double polarization antennas. The signals captured from the antennas are then collected into a processing room which digitizes and processes the data.

As shown in Figure 1 the connection between each antenna and the processing room is performed by exploiting the Radio-over-Fiber (RoF) technique. This technique is generally employed within telecommunications applications for distributing the radio signals (Wi-Fi, 4G, 5G, etc..) from a centralized base station to different Radio Access Points

(RAPs) improving and optimizing the wireless coverage also from cost and consumption point of view. Depending on the scenario, many consolidated configurations exploiting different kinds of fibers (single-mode, multi-mode, plastic) and devices (DFB, VCSELs, etc…) can be utilized [2-5].

In case of SKA radio-telescope, the RoF system which connects each antenna to the central processing room exploits the Wavelength Division Multiplexing (WDM) technique, to separately transmit to the Remote Processing Room the two X and Y linear polarizations of the RF received signal.

A WDM RoF transmitter and a WDM RoF receiver are employed, operating at 1270nm and 1330nm, while the optical fiber used to connect the two devices is the G.652D Standard Single Mode Fiber (SSMF). The two used wavelengths have been chosen around 1310nm, minimizing the effect of chromatic dispersion which could otherwise determine a relatively high instability of the phase difference between the two received polarization signals and among the same polarization received by different antennas.
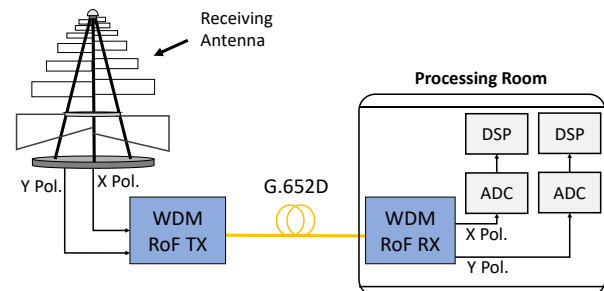

Fig. 1. Illustration of a single RoF link which connects one antenna to the processing room.

In order to analyze all the possible impairments of the technologies on which SKA1-LOW is based, a verification system, named Aperture Array Verification System [6] (currently at version 1.5), composed on a lower number of antennas and links has been first realized. In particular the accurate control of the link non-linearities, which can produce spurious components at the receiver side leading to intra-band distortions terms, is in this context investigated.

Indeed, the signals transmitted in the RoF links are composed of sky signals to which possible RF interfering signals (RFIs) are added. The power levels at which these

signals reach the optical link are relatively low, and negligible impairments are then expected to be generated by possible nonlinear characteristics of lasers and photodiodes. Moreover, the non-linearities produced by chromatic dispersion and frequency chirp [7] feature also a negligible impact at the wavelengths utilized.

However, another phenomenon, namely the Rayleigh Backscattering (RB), can result to be a source of spurious frequency terms in RoF links. This undesired aspect of RB has been given a relatively low attention, if compared with the extensively studied RB-related generation of additional noise in an optical system [8]. This is reasonably due to the fact these RB-related nonlinearities show up in RoF links which feature few km lengths and transmit RF signals of low frequency exhibiting low RF power. These conditions are indeed hardly met together by usual telecommunications RoF links, while they are precisely present in the SKA1-LOW-related ones.

Within this context, the present work describes in detail the distortion effects induced by RB in RoF links, and illustrates from both the theoretical and the practical points of view how, adding a low frequency sinusoidal tone in input to the directly modulated laser, these impairments can be reduced.

The introduction of this so-called *dithering* tone has already been proposed and successfully utilized for the mitigation of the RB-related noise in optical systems [9]. In the present work it is then demonstrated how this same solution can beneficially be applied and optimized for the mitigation of RB-related nonlinearities in RoF systems and how, taking into account some particular physical aspects of these nonlinearities, the efficacy of this solution can be further optimized.

II. SYSTEM AND PHENOMENON DESCRIPTION

A. Experimental Setup and observation of RB

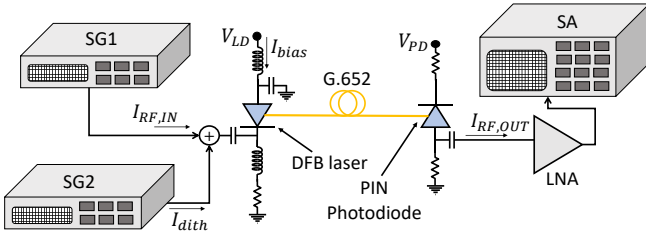The experimental setup utilized for evaluating the RB-induced nonlinearities is presented in Figure 2.

Fig. 2. Experimental setup utilized for the characterization of the optimum frequency and amplitude of the dithering tone to suppress the Rayleigh Backscattering. Signal generator (SG) 1 is used for emulating the RFI tones, while SG2 is used for generating the dithering tone. The harmonics are then measured with a Spectrum Analyzer (SA).

The system is composed of two signal generators, SG1 and SG2, whose outputs are combined and sent to the RF input of the laser. SG1 emits two sinusoidal tones at frequencies $f_{RF,1} = 70$ MHz and $f_{RF,2} = 72$ MHz with power $P_{RF,IN}$ each, while SG2 injects the mentioned dithering tone of frequency f_{dith} ranging in this case from less than 1KHz to 10KHz. Measurements have been performed on the link operating at 1330nm employing a Distributed Feedback (DFB) laser. Its threshold current is $I_{th} = 5$ mA and it is biased at $I_{bias} = 25$ mA, corresponding to an optical transmitted power of about +4 dBm.

The laser is then connected to a span of standard G.652D fiber of which various lengths have been tested. At the receiver side, a PIN photodiode followed by a Low Noise Amplifier (LNA) is used, whose output is connected to a Spectrum Analyzer (SA). To evaluate the nonlinearities of the link, the analysis was focalized the quantity:

$$C/IMD_{f_{RF,1}+f_{RF,2}}[dB] = C[dBm] - IMD_{f_{RF,1}+f_{RF,2}}[dBm] \quad (1)$$

where C is the output power either at frequency $f_{RF,1}$ or $f_{RF,2}$, while $IMD_{f_{RF,1}+f_{RF,1}}$ is the power of the second order intermodulation product, located at 142 MHz.

The impact of RB on $C/IMD_{f_{RF,1}+f_{RF,2}}$ as function of the fiber length is shown in Fig.3 by keeping the input RF power of each tone $P_{RF,IN} = -33$dBm, which corresponds to the order of magnitude of the RFIs present in the SKA1-LOW environment at the input laser section. Note that $C/IMD_{f_{RF,1}+f_{RF,2}}$ decreases with respect to length, in line with the correspondent increase of the RB-related Optical Return Loss (inset of Fig. 3).
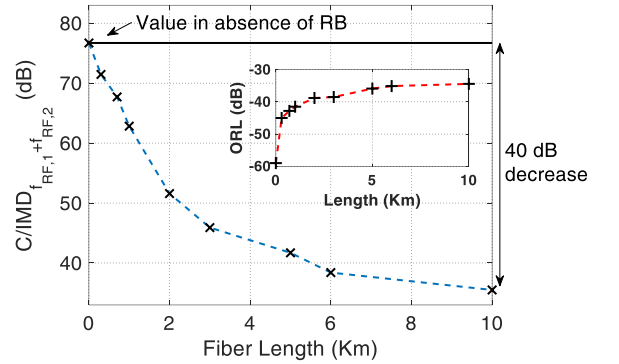

Fig. 3. $C/IMD_{f_{RF,1}+f_{RF,2}}$ for different fiber lengths. As inset, the measured Optical Return Loss (ORL) produced by the RB. ORL is computed normalizing the backscatterd optical power to the injected one.

In order to study this phenomenon and pursue its solution in the worst case, a link length of 10Km has been chosen. This value represents also the current specification for the optical link design of SKA1-LOW.
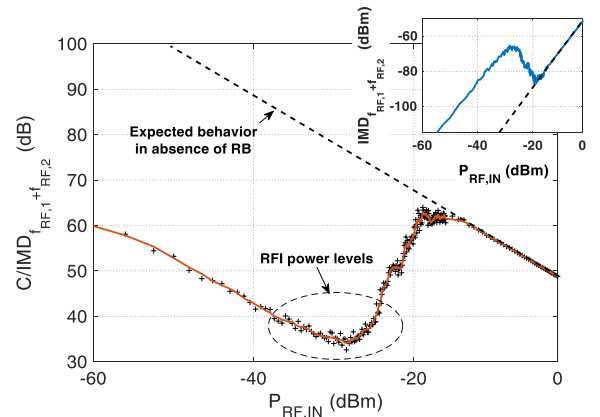

Fig. 4. Behaviors of $C/IMD_{f_{RF,1}+f_{RF,2}}$ and (inset) $IMD_{f_{RF,1}+f_{RF,2}}$ vs. $P_{RF,IN}$. See text for details.

Fig. 4 shows the behavior of the ratio $C/IMD_{f_{RF,1}+f_{RF,2}}$ as a function of $P_{RF,IN}$. Note that, diminishing $P_{RF,IN}$ from 0dBm, the ratio increases, as expected, with unitary slope. However for $P_{RF,IN}$ lower than around -18dBm the ratio starts to exhibit lower values than expected, denoting an undesired

increase of $IMD_{f_{RF,1}+f_{RF,2}}$ (see inset) in the same interval. In the following, both theoretical explanation and proposed solution of the problem will be given.

B. Explanation of the phenomenon

The non-linear effects observed arise from the combination of RB and laser frequency chirp due to the direct modulation of the laser source [10]. For mere simplicity of the mathematical treatment, the following theoretical explanation, instead of deriving the term at $f_{RF,1}+f_{RF,2}$, will consider the term $2f_{RF}$, which shows the same unexpected behavior also in the simpler case where the modulating current consists in one sinusoidal tone with frequency f_{RF}.

The modulating current is in this case $I_{RF,IN}\cos(\omega_{RF}t)$, where $\omega_{RF}=2\pi f_{RF}$, and the expression of the spurious phase modulation term due to the laser chirp results to be $\Delta\theta(t)=M\sin(\omega_{RF}t)$, where $M=K_f I_{RF}/f_{RF}$ and where K_f is the adiabatic chirp factor, which represents the major chirp contribution in DFB lasers [11]. The main component of the electric field $E_{TX}(t)$ emitted by the laser with optical angular frequency ω_0 can be written as:

$$E_{TX} = E_0\sqrt{1+m_{I,RF}\cos(\omega_{RF}t)}\,e^{jM\sin(\omega_{RF}t)}e^{j\omega_0 t} \qquad (2)$$

where E_0 is the field amplitude, while $m_{I,RF}=I_{RF}/(I_{bias}-I_{th})$ is the optical modulation index. Exploiting the Anger-Jacobi expansion of the factor $e^{jM\sin(\omega_{RF}t)}$ it is possible to write equation (2) as sum of Bessel functions as follows:

$$E_{TX} = E_0\sqrt{1+m_{I,RF}\cos(\omega_{RF}t)}\sum_n J_n(M)e^{jn\omega_{RF}t}\,e^{j\omega_0 t} \qquad (3)$$

in which, with the notation $J_n(M)$, the Bessel function of first kind of argument M and of order n is indicated.

Due to RB, portions of E_{TX} can be reflected at different sections of the fiber and produce a feedback into the laser being then re-emitted into the fiber itself. In detail, if no attenuation is assumed for simplicity, the expression of the electric field who arrives to the photodetector is given by the following expression:

$$E_{out}(t) = E_{TX}(t) + E_{BS}(t) = = E_{TX}(t) + \sum_k c_k E_{TX}(t-\tau_k) \qquad (4)$$

where the summation at the last side represents the reflected/re-emitted field $E_{BS}(t)$. This quantity is modelled as the sum of many terms each one of which represents a copy of the initially transmitted field E_{TX} having delay τ_k and coefficient c_k. The generated output current is then given by:

$$i_{out} = R\cdot|E_{out}|^2 = R\cdot[|E_{TX}|^2 + |E_{BS}(t)|^2] + + R\cdot 2\Re\{E_{TX}(t)\cdot E_{BS}^*(t)\} \qquad (5)$$

where R is the responsivity of the detector and the term $|E_{BS}(t)|^2$ can be considered negligible due to its quadratic dependence on the small terms c_k.

After a derivation, which happens to be similar to the one utilized in [12] in a different context, it can be shown that the power of the second order term $P_{2f_{RF}}$ has a behavior proportional to the average performed over the various τ_k's of $J_2^2\left(2M\sin\left(\frac{\omega_{RF}\tau_k}{2}\right)\right)$. As mentioned, it can be derived that the same happens with the term $IMD_{f_{RF,1}+f_{RF,2}}$ analyzed in the previous subsection.

The inset of Fig.4 confirms a J_2^2 -like behavior in correspondence to the RFI's power levels. The mentioned average of $J_2^2\left(2M\sin\left(\frac{\omega_{RF}\tau_k}{2}\right)\right)$ exhibits its higher values when the quantity $M=K_f I_{RF}/f_{RF}$ ranges roughly from 0.4-0.5 up to 1-1.2. Indeed, since for the lasers utilized it is $K_f\sim300\,[MHz\,/mA]$ these are the resulting values of M for the power levels of the RFI, at the frequencies of SKA1-LOW.

Note that, in the hypothesis that the chirp coefficient K_f does not change with frequency, this effect should be also visible for other ranges of values of I_{RF} (proportional to $\sqrt{P_{RF,IN}}$) and f_{RF}, provided that their ratio remains the same as in the SKA1-LOW case. However, thinking about typical telecommunications applications, where the frequencies utilized are of at least few GHz, the appropriate values of M correspond to input powers at least around 20dB higher than the ones considered here. These power levels are generally enough to make the non-linearity of the devices prevail on the ones generated by RB and frequency chirping, practically masking the phenomenon just illustrated.

III. APPLICATION OF THE DITHERING TECHNIQUE

A. Impact on $C/IMD_{f_{RF,1}+f_{RF,2}}$

As anticipated, an efficient way to mitigate this phenomenon is the dithering technique, which determines an enlargement of the laser emission spectrum. The consequent decrease of the laser coherence, results in a reduction of the coherence between $E_{TX}(t)$ and $E_{BS}(t)$ and consequently of the relative weight of the double product of Eq. (5).

Note that the physical effect obtained by applying the dithering tone is the same (frequency chirping) explained in Section II.B. However, the value of the phase modulation index M is much higher due to the inverse proportion with the frequency leading to a more distributed spectrum power along the frequency axis.

The figure below shows the effect on $C/IMD_{f_{RF,1}+f_{RF,2}}$ of the technique applied for different dithering frequencies and amplitudes.
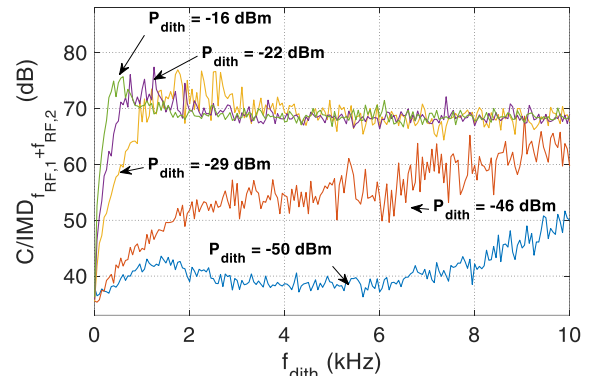

Fig. 5. Effect of dithering tone insertion on the value of $C/IMD_{f_{RF,1}+f_{RF,2}}$ for the 10Km RoF link, measured with $P_{RF,IN}=-33\,dBm$ and varying frequency and amplitude of the dithering tone.

The improvement obtained with dithering frequency and amplitude can be appreciated. Figure 5 suggests that the improvement saturates for both quantities. Values of f_{dith} greater than around 4kHz, choosing values of P_{dith} ranging between around -29dBm and -16dBm brings indeed the system to exhibit an acceptable value of $C/IMD_{f_{RF,1}+f_{RF,2}}\sim70dB$ as opposed to the value of around 38dB shown in Fig.3.

B. Optimum power of the dithering tone

The degree of freedom given to the designer on the choice of the value of P_{dith} can be advantageously exploited to avoid that the dithering tone, in addition to the desired result of reducing the nonlinearities related e.g. to a RFI of frequency f_{RF}, can bring also the presence of high levels of undesired intermodulation terms. In particular, due to the very low value of f_{dith} the most important intermodulation products result to be located in the vicinity of f_{RF}, e.g. at $f_{RF} - f_{dith}$ and $f_{RF} + f_{dith}$. This last component has been considered in the following evaluations.

Theoretically the ratio between the carrier and the intermodulation (namely $C/IMD_{f_{RF}+f_{dith}}$) should depend only on the level of the dithering tone. This can be shown considering again for simplicity the case when only one sinusoidal tone with frequency f_{RF} modulates the laser.

To model the nonlinearities of the second order, the expression of the photodiode output current can be given as:

$$i_{out} = i_{out,0}\{1 + x(t) + a_2[x(t)]^2\} \qquad (6)$$

where

$$x(t) = m_{I,RF} \cos(\omega_{RF}t) + m_{I,dith} \cos(\omega_{dith}t) \qquad (7)$$

and where $m_{I,dith} = I_{dith}/(I_{bias} - I_{th})$, with I_{dith} amplitude of the dithering tone and $\omega_{dith} = 2\pi f_{dith}t$. The coefficient a_2 accounts for the intrinsic second order nonlinearities of the laser and possibly of the photodiode.

The electrical power received at ω_{RF} collected by a resistive load R_L can now be written as:

$$P_{\omega_{RF}} = \frac{1}{2}R_L\big[i_{out,0}m_{I_{RF}}\big]^2 \qquad (8)$$

while for $IMD_{f_{RF,1}+f_{dith}}$ it is

$$P_{IMD_{f_{RF}+f_{dith}}} = \frac{1}{2}R_L\big[i_{out,0}a_2\,m_{I_{RF}}m_{I,dith}\big]^2 \qquad (9)$$

the expression of the ratio $C/IMD2_{f_{RF}+f_{dith}}$ becomes then:

$$\frac{c}{IMD_{f_{RF}+f_{dith}}}[dB] = -20\,log_{10}(a_2 m_{I,dith}) \qquad (10)$$

and, as mentioned, does not depend on the level of the RF signal considered, but only on the dithering amplitude level, proportional to $\sqrt{P_{dith}}$.
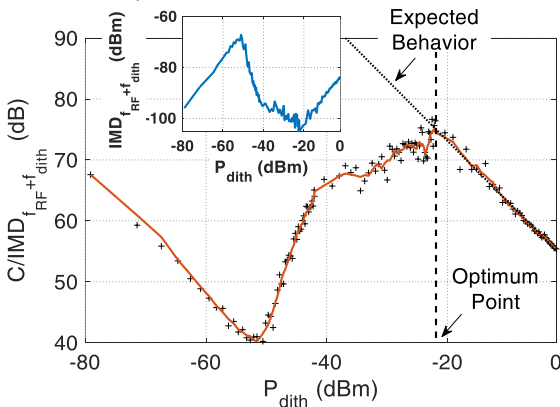

Fig. 6. $C/IMD2_{f_1+f_{dith}}$ vs. P_{dith} with $f_{dith} = 8$ KHz and $P_{RF,IN} = -33$dBm. The ideal behavior is modelled by taking $a_2 = 0.35$.

Fig. 6 shows the behavior of $C/IMD_{f_{RF}+f_{dith}}$ for varying values of the dithering tone power P_{dith}. Note that for relatively high values of P_{dith} (greater than about -20dBm in this case) the model presented in this section fits perfectly the theoretical one confirming the validity of Eq. 10.

On the contrary, for P_{dith} lower than the mentioned value an effect arises similar to the one observed with reference to $C/IMD_{f_{RF,1}+f_{RF,2}}$ (see again Fig.4). This indicates that also in this case the effect of RB dominates, increasing the value of $IMD_{f_{RF}+f_{dith}}$ (see inset of Fig.6). As a results of these considerations, the application of the dithering tone technique allows to identify an optimum value of P_{dith} able to maximizes both $C/IMD_{f_{RF,1}+f_{RF,2}}$ and $C/IMD2_{f_{RF}+f_{dith}}$. In the considered practical case, this value is $P_{dith} = -22dBm$, corresponding to $I_{dith} = 0.5mA$).

IV. CONCLUSION

The distortion introduced by Rayleigh Backscattering has been put into evidence in Radio-over-Fiber links for the Square Kilometer Array Radio-Telescope. An efficient countermeasure based on the introduction of a so-called dithering modulating tone has been proposed and motivated. Through a detailed theoretical and experimental analysis, the values of some operation parameters have been identified. A solution of the kind presented has been effectively installed in the RoF links present in version 1.5 of the Aperture Array Verification System within the SKA project.

REFERENCES

[1] P.Bolli, et al. "From MAD to SAD: The Italian experience for the low-frequency aperture array of SKA1-LOW," Radio Sci., 51, 160–175, March 2016.

[2] J. Nanni, J. Polleux, C. Algani, S. Rusticelli, F. Perini and G. Tartarini, "VCSEL-Based Radio-Over-G652 Fiber System for Short-/Medium-Range MFH Solutions," IEEE/OSA J. Lightw. Technol, vol. 36, pp. 4430-4437, Oct.1, 2018.

[3] J. Nanni, F. Pizzuti, G. Tartarini, J. Polleux and C. Algani, "VCSEL-SSMF-based Radio-over-Fiber link for low cost and low consumption wireless dense networks," Proc. Int. Topical Meeting Microw. Photonics (MWP), Beijing, Oct. 2017.

[4] Y. Shi et al., "Ultrawideband Signal Distribution Over Large-Core POF for In-Home Networks," IEEE/OSA J. Lightw. Technol, vol. 30, pp. 2995-3002, Sept. 2012.

[5] D. Visani, G. Tartarini, M. N. Petersen, L. Tarlazzi and P. Faccin, "Link Design Rules for Cost-Effective Short-Range Radio Over Multimode Fiber Systems," IEEE Trans. Microw. Theory Techn., vol. 58, pp. 3144-3153, Nov. 2010.

[6] P. Benthem et al., "The low frequency receivers for SKA 1-low: Design and verification, " Proc. URSI GASS, Montreal, QC, 2017.

[7] G. Tartarini and P. Faccin, "Efficient characterization of harmonic and intermodulation distortion effects in dispersive radio over fiber systems with direct laser modulation," Microw. Opt. Techn. Lett. Vol 46, pp. 114-117, May 2005.

[8] P. Gysel, R. K. Staubli and R. U. Hofstetter, "Spectral behavior of directly modulated laser diodes exposed to Rayleigh backscatter from a single-mode fiber," IEEE Photon. Technol. Lett., vol. 3, pp. 207–209, March 1991.

[9] S. L. Woodward and T. E. Darcie, "A method for reducing multipath interference noise," IEEE Photon. Technol. Lett., vol. 6, pp. 450-452, March 1994.

[10] A. Villafranca, J. Lasobras and I. Garces, "Precise characterization of the frequency chirp in directly modulated DFB lasers," Proc. Spanish Conf. Electron Devices, Madrid, 2007, pp. 173-176.

[11] J. Nanni et al., "Chirp evaluation of semiconductor DFB lasers through a simple Interferometry-Based (IB) technique," OSA Appl. Opt., vol. 55, pp. 7788-7795 Aug. 2016.

[12] U. Kruger and K. Kruger, "Simultaneous measurement of the linewidth, linewidth enhancement factor α, and FM and AM response of a semiconductor laser, " IEEE/OSA J. Lightw. Technol, vol. 13, pp. 592-597, Apr. 1995.